

Dendrimer templates for heterogeneous catalysts: Bimetallic Pt–Au nanoparticles on oxide supports

Bethany J. Auten, Huifang Lang¹, Bert D. Chandler^{*}

Department of Chemistry, Trinity University, One Trinity Place, San Antonio, TX 78212-7200, United States

Received 8 November 2007; received in revised form 10 December 2007; accepted 12 December 2007

Available online 27 December 2007

Abstract

Polyamidoamine (PAMAM) dendrimers were used to template Pt, Au, and bimetallic Pt–Au dendrimer encapsulated nanoparticles (DENs) in solution. Adjusting the solution pH allowed for slow, spontaneous adsorption of the nanoparticles onto silica, alumina, and titania. After dendrimer removal, the catalysts were characterized with infrared spectroscopy of adsorbed CO and tested with CO oxidation catalysis. Infrared spectroscopy of the monometallic Pt catalysts showed a slight shift in the CO stretching frequency for the different supports. For the bimetallic catalysts, infrared spectra showed CO adsorbed on both Pt and on Au sites. Spectra collected during CO desorption showed substantial interactions between the two bands, confirming the presence of bimetallic particles on all the supports. The bimetallic catalysts were found to be more active than the monometallic catalysts and had lower apparent activation energies. The titania supported Pt–Au catalyst was resistant to deactivation during an extended treatment at 300 °C. Correlations between IR spectra and catalytic activity showed differences between the mono- and bimetallic materials and implicated a bimetallic Pt–Au ensemble at the catalytic active site. This is the first study to show that DENs are appropriate precursors for studying support effects on catalysis by metal nanoparticles, although the magnitude of the effects were small.

© 2008 Elsevier B.V. All rights reserved.

Keywords: Catalyst preparation; Dendrimer encapsulated nanoparticles; PAMAM dendrimers; Pt catalysts; Au catalysts; Pt–Au catalysts; Bimetallic catalysts; CO adsorption; Infrared spectroscopy of adsorbed CO; Nanoparticle preparation; Support effects

1. Introduction

For many supported catalyst systems, particularly Au-based catalysts, the metal-support interface has important influences on catalytic activity [1]. Studying support effects, however, is difficult when catalysts are prepared through traditional impregnation techniques such as incipient wetness impregnation and deposition-precipitation. One of the key barriers to understanding support effects on heterogeneous catalysts is that, when traditional preparation methods are used, nanoparticle preparation occurs on the surface of the support. This makes it extremely difficult to separate the effects of the support during particle formation from the effects of the support on nanoparticle reactivity. In other words, it is difficult to ensure that the catalytically active

particles are comparable from one support to another when the preparation of those catalytically active particles is so closely tied to the support. These inherent problems are further exacerbated for bimetallic catalysts, where differing precursor mobility, compositional inhomogeneity, and new types of active sites substantially complicate the ultimate catalysts. The “simple” preparation of well-defined bimetallic nanoparticle catalysts is a considerable challenge on a single support, and confidently comparing particles on different supports is even more difficult.

Recent advances in solution nanoparticle preparation techniques offer new opportunities for studying heterogeneous catalysts. Of key importance is the ability to separate nanoparticle preparation from support surfaces through wet chemical syntheses. Recent studies have started to evaluate particle size and shape effects on heterogeneous catalyst activity [2–5], but these have not yet been extended to evaluating support effects. Appropriate solution preparation techniques also offer new opportunities for studying composition effects on bimetallic catalysts, particularly for metal

^{*} Corresponding author. Tel.: +1 210 999 7557; fax: +1 210 999 7569.

E-mail address: bert.chandler@trinity.edu (B.D. Chandler).

¹ Present address: Sigma-Aldrich Co., 6000 N. Teutonia Avenue, Milwaukee, WI 53209, United States.

systems that are not thermodynamically stable in the bulk. Separating particle preparation from the support surface is of particular importance for bimetallic catalysts because traditional impregnation techniques do not lead to bimetallic particles for several systems that computational studies have highlighted as systems of interest [6–10].

In particular, supported bimetallic Pt–Au nanoparticles are of fundamental interest and importance. The effects of heterometals (e.g. Pt) on the surface chemistry and catalytic properties of gold based nanoparticles are largely unknown [1]. Further, gold is one of only two transition metals more electronegative than platinum [11], so the incorporation of Au into Pt nanoparticles may have unique effects on catalysis by Pt. Recent interest in supported Pt–Au catalysts has centered on their potential as catalysts for selective oxidation [12,13], dehydrogenation [14], or NO decomposition [15], electrocatalysts [16–19], and selective sensors [20]. Computational studies have also pointed to potentially interesting interactions between Pt–Au surfaces and CO or NO [15,21,22].

The bulk Pt–Au phase diagram has a large miscibility gap extending from 18% to 98% Pt [23,24]. Consequently, most attempts to prepare Pt–Au catalysts using traditional impregnation methods have resulted in phase segregation and catalysts containing large particle agglomerates [12,14,25–28]. Bimetallic Pt–Au nanoparticles have been prepared inside zeolite supercages where the oxide structure arrests particle agglomeration and traps bimetallic nanoparticles [29]. Inorganic and organometallic cluster compounds have also been successful in preparing bimetallic Pt–Au nanoparticle catalysts that show novel reactivity in hydrocarbon conversion reactions and the selective catalytic reduction of nitrogen oxides [12,26,30–35]. Very few appropriate non-phosphine precursors exist for the Pt–Au system; consequently, the cluster route does not allow Pt:Au metal ratios to be varied or tuned [36].

Solution nanoparticle preparation techniques offer new opportunities for studying Pt–Au particles and catalysts. Developing methods for preparing Pt–Au nanoparticles include modifications to the Brust method for synthesizing Au nanoparticles [37–39], co-reduction in the presence of citrate or polymer capping agents [40–45], oil-in-water microemulsions [18,19], and the dendrimer templating method that is the subject of this work [46]. In particular, recent studies from the Nuzzo [47] and [17,38] labs have shown that nanoparticles prepared by such methods may be of compositions throughout bulk miscibility gaps. These preparative techniques have largely been developed by researchers whose primary interests are in areas far afield from heterogeneous catalysis; consequently, there are few reports of their application to catalyst preparation. One report is available on homogeneous allyl alcohol hydrogenation [42], while several studies have focused on electrocatalysis [17–19,39,48,49]. Only two studies detail heterogeneous CO oxidation [46] and naphthalene hydrogenation [43] catalysis by supported Pt–Au particles prepared with these new methods.

We have been developing a nanoparticle catalyst preparation method using polyamidoamine (PAMAM) dendrimers as

nanoparticle templates/stabilizers for Pt [50–53], Au [54,56], and Pt–Au [46] catalysts. Our previous work showed that Pt and Pt–Au dendrimer encapsulated nanoparticles (DENs) can be prepared in solution and deposited on to high surface area silica via spontaneous adsorption. We, and others, also showed that calcination and/or reduction treatments can be used to remove the dendrimer templates while maintaining the bimetallic nature of the nanoparticles and without sintering the metals into large agglomerates [46,50–53,56–59]. Further, Pt–Au nanoparticles can be prepared on a commercial silica using metal ratios within the miscibility gap and not attainable via cluster precursors [46].

The goal of this study was to determine if DENs are appropriate precursors for studying support effects for nanoparticle catalysts. Because nanoparticles in DENs are prepared in solution, they can be deposited onto a variety of substrates, potentially without changing the particle properties. Pt–Au nanoparticles are a good system for evaluating these effects because bimetallic nanoparticles cannot be prepared via traditional methods. Further, when bimetallic interactions are maintained, enhanced CO oxidation activity is observed and spectroscopic characterization of Au surface sites with infrared spectroscopy of adsorbed CO is possible. Additionally, this study provides an initial opportunity to investigate the magnitude support effects on Pt–Au catalysts.

2. Experimental

2.1. Materials

All solutions were prepared using water purified to a resistivity of 17–18 M Ω /cm with a Barnstead Nanopure system. Hydroxyl-terminated generation five starburst PAMAM dendrimers (G5-OH) were obtained as a 5% solution in methanol (Aldrich). Prior to use, methanol was removed by rotary evaporation at room temperature. K₂PtCl₄, NaBH₄ and Cu(NO₃)₂ were purchased from Aldrich and used without further purification. HAuCl₄ was obtained from Strem Chemicals. Silica (DAVICAT SI – 1403, 245 m²/g; pore volume = 2 mL/g) was supplied by W.R. Grace. γ -Al₂O₃ (PURALOX HP 14/150, 150 m²/g; pore volume = 0.958 mL/g; γ -Al₂O₃) was supplied by SASOL. The titanias (AEROLYST 7711, i.e. Degussa p-25 or p₂₅TiO₂ and AEROLYST 7709, i.e. amorphous TiO₂ or am-TiO₂) were provided by Degussa Corporation. O₂, H₂, He gasses were all UHP grade from Airgas. Carbon monoxide (99.8% in aluminum cylinder) was purchased from Matheson Tri-Gas.

2.2. Nanoparticle preparation, deposition, and dendrimer removal

The preparation detail of monometallic dendrimer encapsulated Pt and Au nanoparticles, as well as the preparation of bimetallic Pt–Au nanoparticles via Cu-exchange was previously reported [46]. Briefly, G5-OH(Cu)₄₀ dendrimer encapsulated nanoparticles are prepared by complexing 40 equivalents Cu²⁺ to 0.2 μ M G5-OH PAMAM dendrimer,

followed by reduction with NaBH_4 . The solution pH was adjusted to 3 to hydrolyze excess NaBH_4 and then returned to pH 7. Appropriate volumes of 5 mM K_2PtCl_4 and 2 mM HAuCl_4 were degassed separately, mixed, and immediately added to the $\text{G5-OH}(\text{Cu})_{40}$ solution. Supported monometallic Pt and Au DENs were prepared in a similar fashion. For Pt_{32} , 0.2 μmol $\text{G5-OH}(\text{Cu})_{32}$ were prepared and reacted with 5 mM K_2PtCl_4 solution. To make Au_{32} nanoparticles 2 mM HAuCl_4 solution was mixed with 0.2 μmol $\text{G5-OH}(\text{Cu})_{48}$. After stirring for 1 h, the resulting noble metal dendrimer encapsulated nanoparticles were deposited onto the supports. Deposition was achieved by stirring the as-prepared nanoparticles with each support overnight at an appropriate pH (see Table 1).

The solids were isolated and the wet solid catalysts were stirred with saturated EDTA solution at pH 7.0 to remove residual Cu^{2+} . The supported DENs were then dried in a vacuum oven at 50 °C overnight. Dendrimer removal was achieved by calcination at 300 °C for 4 h followed by reduction at 300 °C under H_2 for 2 h [46,50]. Overall metal yields were generally 70–75% and residual Cu^{2+} was always less than 0.01% for the activated catalysts.

2.3. Pt and Au analysis with atomic absorption spectroscopy

Catalyst Pt and Au loadings were determined with a Varian SpectraAA 220FS atomic absorption spectrometer using an acetylene/air flame, as described previously [46,50]. AA standards were prepared from Aldrich AA standard solutions. Samples were dissolved in freshly prepared *aqua regia* and neutralized with ammonium hydroxide. The resulting solution was condensed and transferred to a 10 mL volumetric flask. For Pt containing samples, the volumetric flask contained sufficient $\text{La}(\text{NO}_3)_3$ to yield a final solution of 1% La.

2.4. In situ FT-IR experiments

FT-IR spectra were collected using a Thermo Nicolet Nexus 470 spectrometer equipped with a DTGS detector using a resolution of 2 cm^{-1} . A water-cooled stainless steel IR flow cell with NaCl windows [50] was used to hold a pressed catalyst wafer (SiO_2 : 18–20 mg; Al_2O_3 : 18–20 mg; and TiO_2 : 48–50 mg). All spectra were collected with gasses flowing at 30 mL/min. Gas composition was manipulated by adjusting rotameters on an external manifold.

Table 1
Metal loadings for DEN based catalysts

Support	Deposition pH	Catalyst metal loading(s)		
		Pt (%)	Au (%)	Pt–Au (%)
SiO_2	8–8.5	0.25	0.25	0.16 Pt, 0.14 Au
Al_2O_3	7–8	0.18	0.30	0.40 Pt, 0.42 Au
am TiO_2	6–7	0.14	0.07	0.17 Pt, 0.16 Au
p25 TiO_2	6–7	0.15	0.09	0.17 Pt, 0.16 Au

2.5. CO oxidation

The feed and reactor effluent composition was monitored with a SRI 8610C Gas Chromatograph using a TCD detector, as previously described [50]. To increase sensitivity, the GC gas sample loop was replaced with a 5 mL loop and the gas delivery manifold was rebuilt with low flow (2–20 mL/min) rotameters. Catalyst samples (15 mg) were diluted 10:1 with $\alpha\text{-Al}_2\text{O}_3$ and placed in a single pass plug flow microreactor. The catalyst was then oxidized with O_2 (27% in He) for 4 h and then reduced with H_2 (27% in He) for 2 h at 300 °C. The feed composition (1.1% CO, 27% O_2 balance He) and the total flow rate (20 mL/min) were kept constant during all experiments. Conversion was measured as a function of temperature to obtain rate data, which was reported only when the conversion was below 12%. For stability tests, the bimetallic catalysts were oxidized for an additional 16 h at 300 °C with 27% O_2 , and the light-off curve was repeated.

3. Results and discussion

3.1. Nanoparticle preparation and deposition

One of the primary advantages of the dendrimer route to supported catalysts is that it separates nanoparticle preparation from surface segregation and mobility issues that are inherent to impregnation techniques. This is especially important for evaluating support effects since there is no guarantee that similar particles are prepared on different supports. Our previous work showed that bimetallic Pt–Au nanoparticles can be prepared in solution and deposited onto silica [46]. After thermal activation, the bimetallic nanoparticles were shown to have surface Pt and Au sites and enhanced activity in CO oxidation catalysis. In this work, methods for depositing these nanoparticles onto additional oxide supports (alumina and titania) were determined, and their catalytic activity was examined.

DENs tend to agglomerate in solution unless low concentrations (<50 μM) are maintained [60], making wetness impregnation techniques undesirable. Consequently, conditions where DENs spontaneously adsorb onto alumina and titania were initially determined. Freshly prepared Pt DENs were stirred overnight with each oxide support at an appropriate pH (see Table 1) until the solution turned clear.

Control experiments using PAMAM dendrimers without nanoparticles showed no adsorption onto any of the oxides using dilute solutions of G5-OH dendrimers. These results indicate that the spontaneous adsorption processes observed for DENs are driven primarily by nanoparticle-support interactions rather than dendrimer-support interactions. Adjusting the solution pH increases the overall surface negative charge on the supports, improving their ligand properties, and apparently strengthening the metal-support interactions [61,62]. Strongly binding ligands such as long-chain thiols are capable of removing nanoparticles from aqueous DENs in organic solution, so interactions between the nanoparticles in DENs and functional groups at or near the dendrimer periphery has

substantial literature precedent [54,55,63,64]. Because deposition occurs at neutral or basic pH, both the dendrimer surface groups and the oxide surfaces will have net negative charges, making it unlikely that dendrimer-support interactions drive the adsorption. Additionally, our group and Williams and co-workers have examined PAMAM dendrimers supported on various oxides (silica, alumina titania, zirconia) with infrared spectroscopy [50,51,53,65,66]. In all these studies, the dendrimer could only be deposited through wetness impregnation or by slowly evaporating the solvent, indicating that the dendrimer-support interactions are minimal at the concentrations used in nanoparticle synthesis.

Based on the common preparation procedures described previously for Pt, Au, and Pt–Au DENs, and using the deposition conditions appropriate to each support, a series of Pt, Au, and Pt–Au supported catalysts were prepared (Table 1). All the supported DENs were subjected to high temperature oxidation and reduction treatments (O_2 at 300 °C for 4 h, followed by H_2 at 300 °C for 2 h) to remove the organic material. Our group and others have performed a number of studies on dendrimer thermolysis, and these activation conditions have been shown to remove the dendrimer from supported Pt DENs without causing widespread particle agglomeration [46,50–52,56,57,59,65].

3.2. Infrared spectroscopy of monometallic catalysts

Infrared spectroscopy of adsorbed CO is a rapid characterization tool for the Pt–Au metal system because bimetallic Pt–Au nanoparticles show significant spectral differences relative to monometallic catalysts [17,26,46,67,68]. Because platinum and gold surface atoms are readily distinguished by the stretching frequency of adsorbed CO, IR spectroscopy can therefore be used to confirm the presence of bimetallic nanoparticles. It is also potentially useful as an indicator for detecting differences in metal-support interactions that may modulate supported catalyst properties. Fig. 1 shows IR spectra of CO bound to Pt/ Al_2O_3 , Pt/ $_{am}TiO_2$, and Pt/ $_{p25}TiO_2$. All three catalysts show a strong absorption band in the 2082–2086 cm^{-1}

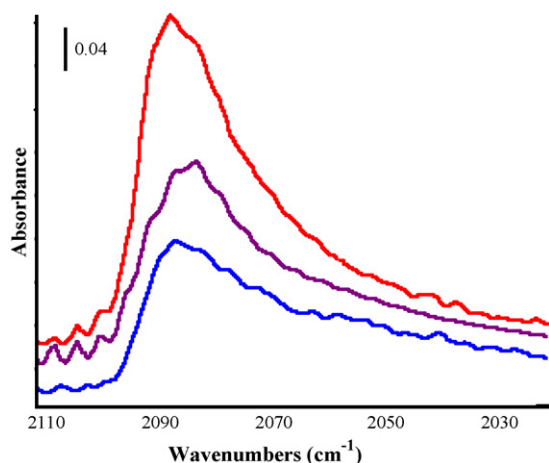


Fig. 1. FT-IR spectra of CO adsorbed on Pt₃₂ NPs supported on am-TiO₂ (top), Al₂O₃ (middle), Degussa p-25 TiO₂ (bottom).

region. The asymmetry of the Pt/ $_{p25}TiO_2$ spectrum suggests that there is greater inhomogeneity in the particle-support interactions on P-25 titania, which is not surprising given that P-25 is a mixture of the anatase and rutile titania polymorphs.

Infrared spectra collected during CO desorption experiments were generally similar for the Pt catalysts, and were comparable to those for silica (see Supporting Information) [46]. All the catalysts showed a 15–20 cm^{-1} red shift in the CO stretching frequency over the course of the desorption experiment. Additionally, complete CO desorption from the monometallic Pt catalysts required heating the IR cell to 180–200 °C. All of the IR data are consistent with dendrimer derived Pt catalysts on silica supports [46,50,69] as well as with supported Pt catalysts prepared with conventional techniques [70].

The IR spectra of CO bound to Au/ $_{p25}TiO_2$ and Au/ $_{am}TiO_2$ show a broad, weak, but discernable higher energy absorption band centered around 2120 and 2125 cm^{-1} , respectively (see Supporting Information). These values are consistent with CO on Au surface sites [1]. The CO giving rise to this band is bound weakly to the surface and desorbs at room temperature with continued He purge. CO adsorption on Au/Al₂O₃ was too weak to detect, similar to the Au/SiO₂ catalysts prepared via this method [46].

Although the synthetic technique used in this study prepares relatively small bimetallic nanoparticles, it is not the most effective means of preparing monometallic Pt or Au catalysts from DENs. Alternate solution syntheses allow for excellent control over particle size and distribution for both metals [71,72] and active gold catalysts can be prepared using modified preparations [55,73]. These monometallic catalysts, however, were prepared expressly as controls for the bimetallic Pt–Au catalysts, for which the Cu displacement technique is well suited. Consequently, the synthesis is not optimized for the monometallic materials and it is not appropriate to undertake an in-depth evaluation of the differences between them.

3.3. Infrared spectroscopy of bimetallic catalysts

Fig. 2 shows FT-IR spectra of CO adsorbed on Pt–Au bimetallic nanoparticles supported on alumina, amorphous TiO₂, and Degussa P-25 titania. Data for the two major adsorption bands are also compiled in Table 2. All the spectra contain a moderately intense high energy adsorption band (2113–2119 cm^{-1}), consistent with CO bound to Au surface sites [12,14,30]. The peaks on the bimetallic catalysts are substantially larger than the surface peaks for the monometallic Au/ $_{p25}TiO_2$ and Au/ $_{am}TiO_2$ catalysts and are red-shifted relative to the control materials. The Au–CO surface peaks slowly disappear with continued purging (He) at room temperature, indicating CO is weakly bound to surface Au sites. The stronger, lower energy absorption bands in Fig. 2 are similar in intensity to the monometallic Pt catalysts and are assigned as Pt–CO bands (see also Table 2). The bimetallic Pt–CO bands are all red-shifted approximately 10 cm^{-1} from the corresponding monometallic catalyst. As with the monometallic Pt/ $_{p25}TiO_2$ catalyst, Pt–Au/ $_{p25}TiO_2$ shows a substantially

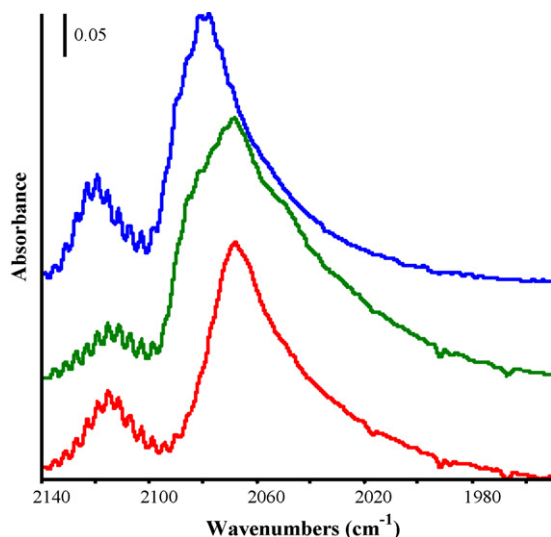


Fig. 2. FT-IR spectra of CO adsorbed on Pt₁₆Au₁₆ NPs supported on Al₂O₃ (top), Degussa p-25 TiO₂ (middle), and am-TiO₂ (bottom).

broader peak for adsorbed CO than the other (amorphous) supports.

Figs. 3–5 show changes in the Pt–Au catalysts' infrared spectra during CO desorption experiments. Upon heating, CO initially desorbs from the Au sites between 80 and 100 °C. The disappearance of the Au–CO band coincides with a further 5–10 cm^{−1} red shift in the Pt–CO band position (Table 2) and an increase in the Pt–CO band intensity. These changes in the Pt–CO band were always concurrent with changes in the Au–CO band.

Although dendrimer templates can be used to prepare bimetallic particles in solution, it is important to confirm that particles remain bimetallic after dendrimer removal. The presence of the Au–CO band, the red shift in the Pt–CO band in

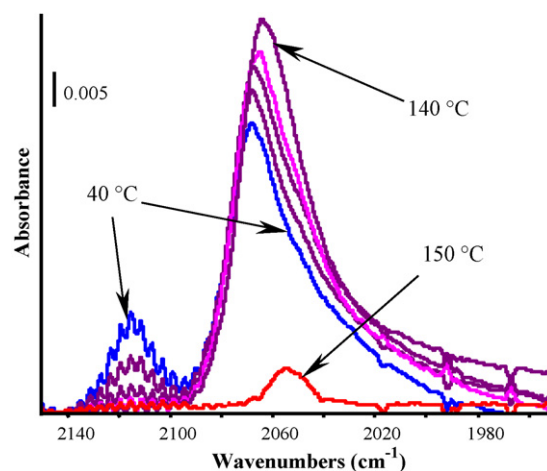


Fig. 3. FT-IR spectra during CO desorption from Pt₁₆Au₁₆ supported on Al₂O₃. Temperatures are: 40 °C (blue), 60, 70, 90, 140, and 150 °C (red). (For interpretation of the references to color in this figure legend, the reader is referred to the web version of the article.)

the full coverage spectra, and the changes in Pt–CO band intensity increase upon CO desorption from Au support confirm that bimetallic nanoparticles are present after dendrimer removal. These changes were previously correlated with high resolution TEM and single particle EDS studies on silica supported Pt–Au nanoparticles [46]. Control experiments using

Table 2
Stretching frequency (in cm^{−1}) data summary for CO adsorbed on the catalysts

Support	Monometallics		
	Au ₃₂ ^a	Pt ₃₂ (high) ^b	Pt ₃₂ (low) ^c
SiO ₂ ^d	–	2081	2075
Al ₂ O ₃	–	2082	2052
am-TiO ₂	2119	2086	2063
p25-TiO ₂	2115	2082	2066
Support	Bimetallics		
	Au ^e	Pt (high) ^f	Pt (low) ^g
SiO ₂ ^d	2113	2063	2052
Al ₂ O ₃	2115	2076	2054
am-TiO ₂	2119	2068	2072
p25-TiO ₂	2115	ca. 2069	ca. 2062

^a $\nu(\text{CO})$ in cm^{−1}.

^b $\nu(\text{CO})$ on Pt in cm^{−1} at high coverage.

^c $\nu(\text{CO})$ on Pt in cm^{−1} at low coverage.

^d From ref. [44].

^e $\nu(\text{CO})$ on Au sites in cm^{−1}; peak positions did not measurably shift during desorption.

^f $\nu(\text{CO})$ on Pt sites in cm^{−1} at high coverage.

^g $\nu(\text{CO})$ on Pt sites in cm^{−1} at low coverage.

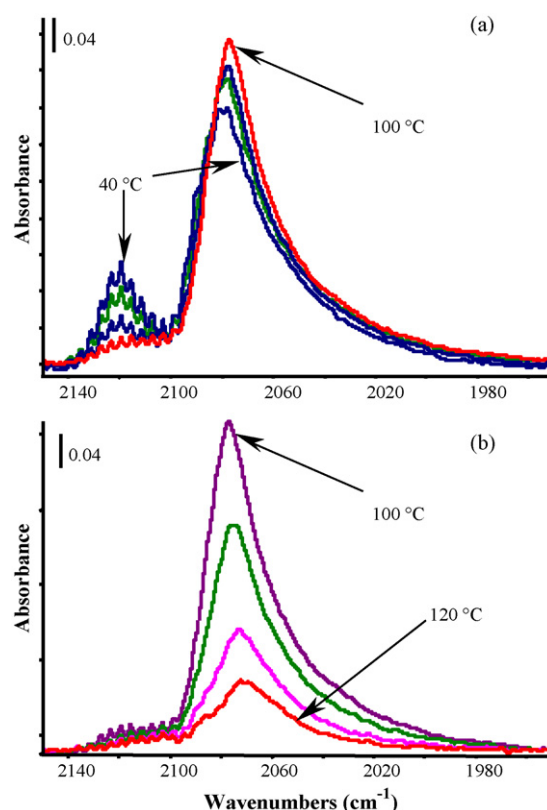


Fig. 4. FT-IR spectra during CO desorption from Pt₁₆Au₁₆ supported on amorphous TiO₂. Temperatures are: (a) 40 °C (blue), 60, 80 and 100 °C (red) and (b) 100 °C (top, purple), 110, 115 and 120 °C (bottom, red). (For interpretation of the references to color in this figure legend, the reader is referred to the web version of the article.)

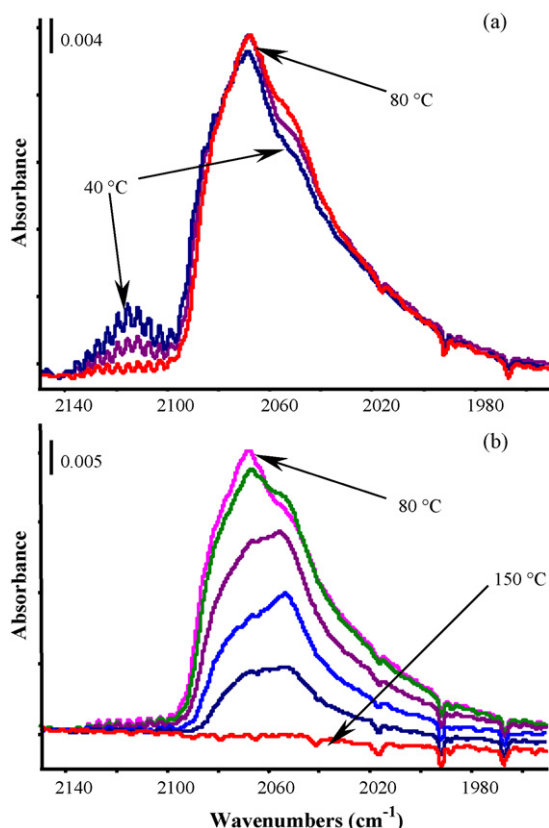


Fig. 5. FT-IR spectra during CO desorption from $\text{Pt}_{16}\text{Au}_{16}$ supported on Degussa p-25 TiO_2 . Temperatures are: (a) 40 °C (blue), 60 and 80 °C (red) and (b) 80 °C (top, pink), 100, 110, 120, 130 and 150 °C (bottom, red). (For interpretation of the references to color in this figure legend, the reader is referred to the web version of the article.)

co-deposited monometallic Pt and Au DENs on silica showed no comparable interactions during CO desorption experiments; i.e. there was no interaction between spectroscopic bands arising from separate monometallic Pt and Au nanoparticles on the same support [46].

The shifts in CO stretching frequency are readily explained with traditional models. The physical separation of diluted Pt–CO dipoles would reduce their ability to participate in dipole coupling, resulting in an apparent red shift relative to a pure Pt surface [70]. Since dipole coupling only occurs between dipoles oscillating at the same frequency [70,74], Au–CO dipoles serve to shield Pt–CO dipoles from one another, and vice versa. This red shift has been previously observed in cluster-derived bimetallic Pt–Au catalysts that have been fully characterized to contain Pt and Au intimately mixed within individual particles [12], and is consistent with previous studies using traditionally prepared Pt–Cu catalysts [74,75].

The literature provides two possible explanations for the changes in the Pt–CO band during CO desorption from Au: spectral intensity redistribution and particle restructuring during heating (perhaps induced by CO). Similar to the dipole coupling interactions, intensity redistribution can arise from the screening of electric fields from lower frequency oscillators, resulting in enhanced absorption by higher frequency bands [76]. Thus, as the higher energy bands are removed during

heating, the intensity borrowing from Pt–CO would diminish, increasing the intensity of the Pt–CO band. Alternately, but a simple surface rearrangement associated with heating the particles might also give rise to the observed changes. CO induced restructuring has been proposed for dilute, thermodynamically stable alloys of Pt in Au prepared by traditional means [14,23] and such restructuring is consistent with the facile exchange of surface and subsurface Pt atoms suggested by Somorjai et al. [77]. Both of these explanations are consistent with the IR data, and both explanations require intimate mixing of the metals.

3.4. CO oxidation by monometallic catalysts

Fig. 6a shows CO oxidation catalysis by Pt nanoparticles on the four metal oxide supports. All of the monometallic Pt catalysts have relatively similar activities, with $\text{Pt}/\text{p}_{25}\text{TiO}_2$ showing the highest activity. Pt/amTiO_2 is similar to Pt/SiO_2 ; both are slightly less active than $\text{Pt}/\text{p}_{25}\text{TiO}_2$. $\text{Pt}/\text{Al}_2\text{O}_3$ is the least active of the monometallic Pt catalysts, exhibiting rates

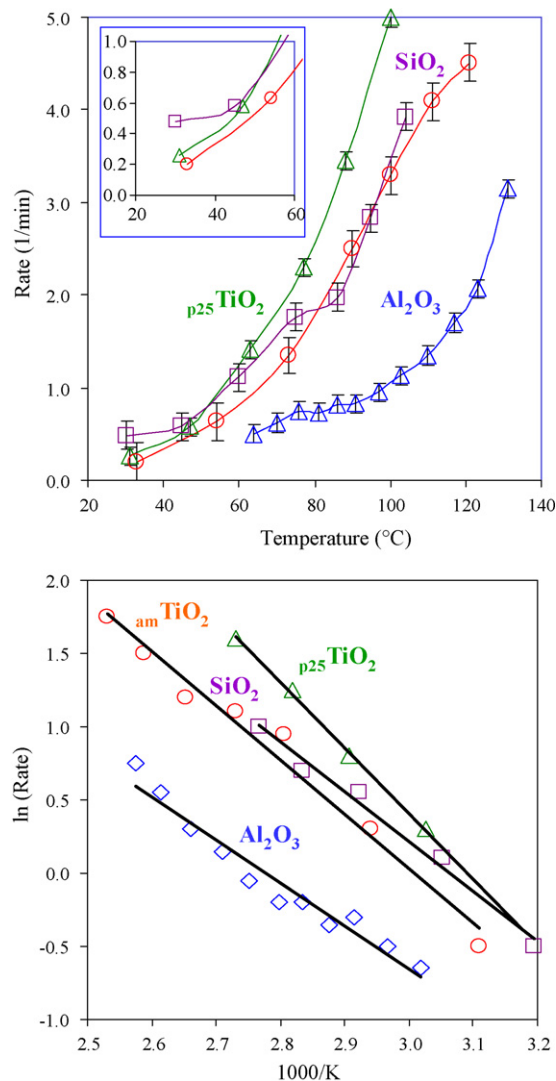


Fig. 6. CO oxidation catalysis data of Pt catalysts supported on Al_2O_3 , SiO_2 , amTiO_2 , and $\text{p}_{25}\text{TiO}_2$ (a) rate versus temperature plot and (b) Arrhenius plot.

Table 3

Apparent activation energies (E_{app}) for dendrimer templated Pt, Au, and Pt–Au catalysts

Support	E_{app} (kJ/mole)		
	Pt	Au	Pt ₁₆ Au ₁₆
SiO ₂	26	85	21
Al ₂ O ₃	33	45	16
amTiO ₂	32	79	29
p ₂₅ TiO ₂	36	82	20

roughly one third of Pt/p₂₅TiO₂. Additionally, all the Pt catalysts have similar responses to temperature changes, which were quantified using Arrhenius plots of rate data between 2 and 12% conversion (Fig. 6b). The slopes of the Arrhenius plots for the supported Pt catalysts are similar and the extracted apparent activation energies (E_{app}) are near 32 kJ/mole (see Table 3).

The activated Pt catalysts have very similar activities, indicating that support effects on the Pt catalysts are relatively small. The magnitude of the observed reactivity differences is consistent with other reports of support effects on CO oxidation by Pt [78]. Based on these data, three reasonable conclusions can be drawn: (i) catalysis occurs on the metal, (ii) the reaction mechanism is similar or the same over all four Pt catalysts, (iii) the support plays a minimal role in modifying Pt activity. The absence of a dramatic increase in activity or change to E_{app} for the TiO₂ supported catalysts suggests that TiO₂ does not donate activated O₂ that might assist in the reaction. If activated O₂ was important for Pt/amTiO₂ or Pt/p₂₅TiO₂, larger changes in the catalytic activities or E_{app} for these materials would be expected.

Fig. 7a shows the rate versus temperature plots for CO oxidation catalyzed by activated Au nanoparticles on the four supports. These materials are essentially inactive at ambient temperatures and none of them showed the high activity that characterizes the most active gold catalysts. Arrhenius plots for the four supported Au catalysts are shown in Fig. 7b. The extracted apparent energies in Table 3 for monometallic gold catalysts were generally around 80 kJ/mol. The large apparent activation energies are consistent with the substantial sintering observed for Au/SiO₂ [1,46]. The preparation and activation protocol used for these studies is appropriate for bimetallic catalysts; however, it does not prepare highly active Au catalysts. Consequently, although these are important control materials, conclusions regarding the nature of any support effects for these catalysts are not warranted.

3.5. CO oxidation by bimetallic catalysts

Fig. 8 provides rate versus temperature plots for the Pt/p₂₅TiO₂, Au/p₂₅TiO₂, and Pt–Au/p₂₅TiO₂ catalysts; it shows that the Pt–Au/p₂₅TiO₂ catalyst is more active than either of the monometallic catalysts. Similar synergy was observed for the bimetallic nanoparticles on all four metal oxide supports (Al₂O₃, SiO₂, p₂₅TiO₂, and amTiO₂ plots are available in the supplementary material). The thermal stability of the bimetallic

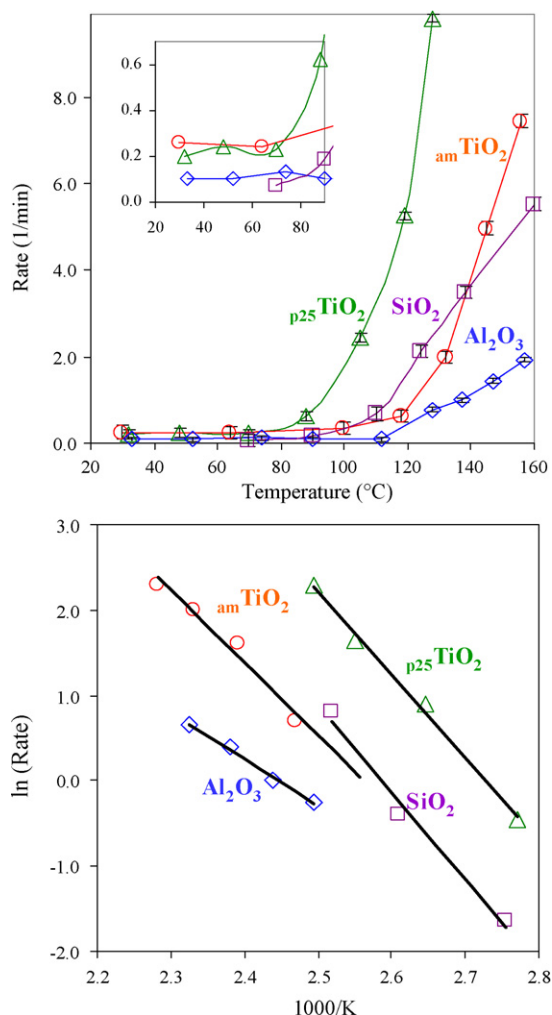


Fig. 7. CO oxidation catalysis data of Au catalysts supported on Al₂O₃, SiO₂, amTiO₂, and p₂₅TiO₂. (a) rate versus temperature plot and (b) Arrhenius plot.

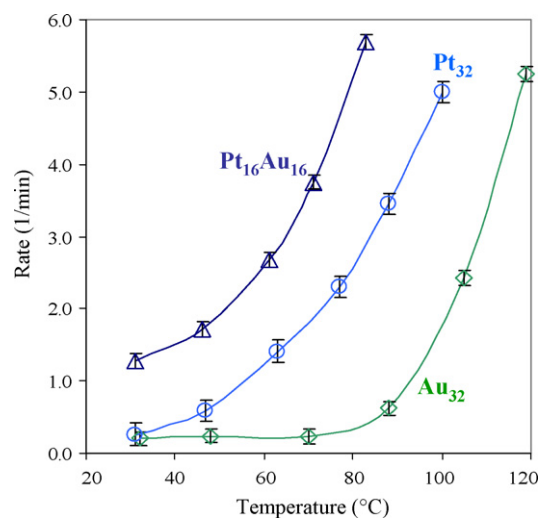


Fig. 8. CO oxidation catalysis data comparing Pt–Au/p₂₅TiO₂ with Pt/p₂₅TiO₂ and Au/p₂₅TiO₂ catalysts.

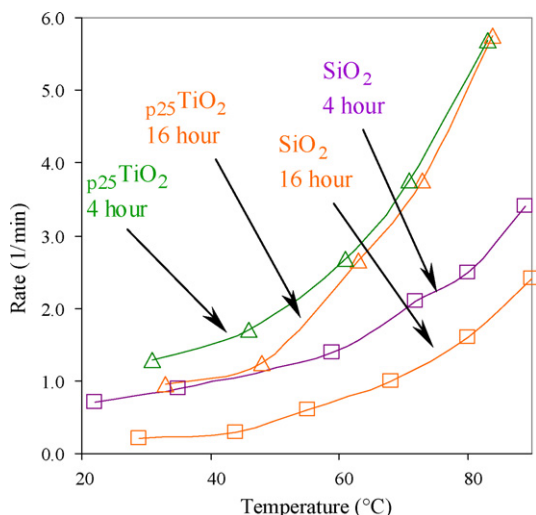


Fig. 9. Comparison of CO oxidation reactivity after 4 h and additional 16 h oxidation treatments for Pt–Au/ $p_{25}\text{TiO}_2$ and Pt–Au/ SiO_2 .

catalysts has not been previously examined, so each catalyst was subjected to an additional 16-h calcination at 300 °C. The results of catalytic activity tests before and after the 16-h treatment are shown for Pt–Au/ $p_{25}\text{TiO}_2$ and Pt–Au/ SiO_2 in Fig. 9. Results for Al_2O_3 and amTiO_2 are similar to SiO_2 and are provided in the supplementary material. The Pt–Au/ $p_{25}\text{TiO}_2$ shows only a small activity loss after the extended oxidation treatment. The bimetallic catalysts on amTiO_2 , Al_2O_3 , and SiO_2 show somewhat greater activity losses, but still retain some activity.

Reaction rates for the bimetallic catalysts are expressed in terms of total moles of Pt for several reasons, but primarily to facilitate comparisons between the mono- and bimetallic catalysts. Studies on supported Pt–Au catalysts have indicated that exchange between surface and subsurface atoms caused by strongly binding ligands may be important for this metal system [14,46]. This means that chemisorption measurements of Pt surface concentrations may be misleading if the particle surface differs between the reaction conditions and the chemisorption experiment. Consequently, in order to avoid making undue assumptions about the surface stoichiometry under the reactive atmosphere, it is most appropriate to express rates in terms of the total amount of metal in each catalyst.

Based on the total amount of metal in the catalysts, four limiting cases for CO oxidation catalysis are possible for the Pt–Au materials. If all of the activity of the bimetallic catalyst is due to either Pt or Au monometallic sites, then a maximum number of active sites are assumed when the rate is corrected for total moles of Pt. Atomic weights of Pt and Au differ by only 1%, so the rate per Pt is essentially the same as the rate per Au with this correction. The choice of a 1:1 Pt:Au ratio also makes direct comparisons to the monometallic control materials relatively straightforward. If the reaction depends on a bimetallic site, then these sites are limited by the total number of Pt (or Au) sites, so correcting by moles of Pt still assumes a maximum number of possible sites.

A fourth possibility is that the reaction depends only on the total number of metal atoms. Correction for total metal

inherently assumes the Pt and Au are equivalent catalysts in these materials. This treatment would require that, in the bimetallic catalyst, both metals generate active sites that perform the reaction at the same rate. This is clearly not the case for the Au and Pt monometallic catalysts. It is unlikely that the two metals become catalytically equivalent when present in bimetallic nanoparticles and we therefore discount this possibility. Consequently, all rates are normalized to the total amount of Pt in the catalyst. This is done primarily out of convenience for comparing the mono- and bimetallic catalysts and is not meant to imply that Pt is the only or even the primary active component in the bimetallic catalysts.

The Pt–Au catalyst activities were relatively similar, as shown in Fig. 10a. Pt–Au/ $p_{25}\text{TiO}_2$ was the most active, Pt–Au/ amTiO_2 and Pt–Au/ SiO_2 have similar activities, and Pt–Au/ Al_2O_3 was the least active of the bimetallic catalysts. The bimetallic catalysts show the same general trend in activity as the monometallic catalysts. The bimetallics are slightly more sensitive to the support choice, but differences are still relatively small. Arrhenius plots (Fig. 10b) show the catalysts

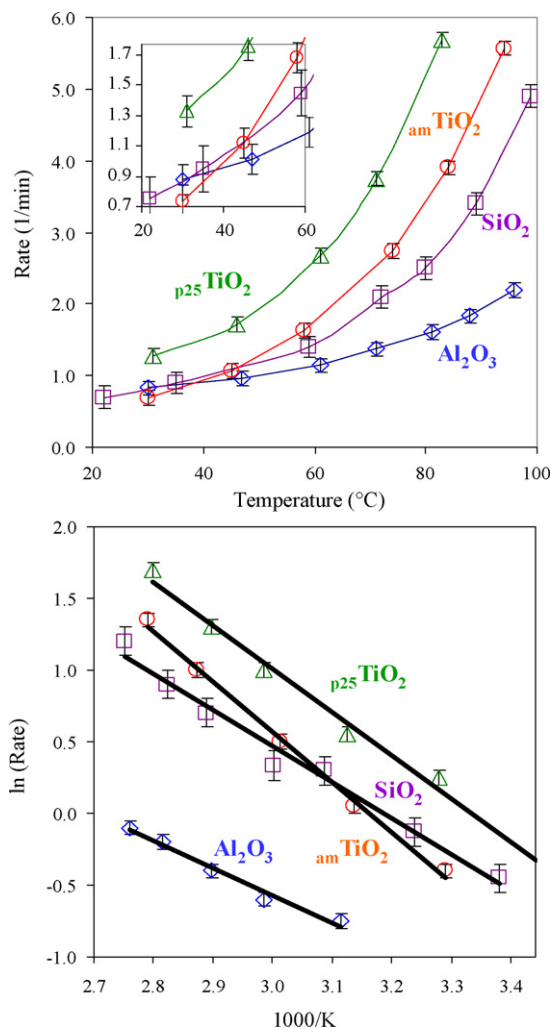


Fig. 10. CO oxidation catalysis data of Pt–Au catalysts supported on Al_2O_3 , SiO_2 , amTiO_2 , and $p_{25}\text{TiO}_2$. (a) rate versus temperature plot and (b) Arrhenius plot.

to have apparent energies near 22 kJ/mol (Table 3). E_{app} values for the bimetallic catalysts are somewhat lower than either monometallic system, and bimetallic catalyst activities were always greater than either of the monometallic catalysts at the temperatures studied. The similarities in the CO oxidation rates and the E_{app} values for the Pt–Au catalysts indicate that particles and the reaction mechanism are not substantially different for these materials. As with the monometallic Pt catalysts, the support appears to play only a small role in modulating the catalytic activity.

Amiridis and co-workers recently reported on CO oxidation catalysis by titania supported Pt–Au nanoparticles prepared from a bimetallic cluster precursor [34]. As with our studies, the titania supported cluster-derived catalyst showed higher activity than traditionally prepared monometallic catalysts. The reaction rates extracted from their light-off curve data at ca. 40 °C (1–3 min^{−1}, depending on pretreatment) are very similar to those for our titania catalysts (1–1.5 min^{−1} at 40 °C). Amiridis' and co-workers studies employed higher conversions than ours, and the organometallic cluster they used has a different Pt:Au ratio (1Pt:2Au). Given the differences in preparation methods, metal ratio, and measurement techniques, there is excellent agreement between our titania supported catalysts and their materials.

In contrast to our studies with dendrimer templated nanoparticles [46], cluster-derived bimetallic catalysts on silica resulted in substantially less active catalysts [34]. Both our catalysts and theirs show similar IR spectra, particularly the ability to weakly chemisorb CO on Au sites [79]. Bus and van Bokhoven have also used X-ray spectroscopy to investigate catalysts derived from silica and titania supported clusters [80,81]. Their results indicate that bimetallic nanoparticles are present on both supports after activation, but that particles show differing degrees of metal–metal mixing. Silica supported nanoparticles appeared to be well mixed while titania supported particles showed some degree of phase segregation within individual particles [80]. Our current study, which shows relatively small activity differences between silica and titania supported catalysts prepared using dendrimer templates, does not shed light onto the differences reported by Amiridis and co-workers. However, it does highlight a potential advantage of using nanoparticles, which contain tens or hundred of atoms, over clusters, which contain several atoms. Although organometallic clusters have a more precisely defined metal stoichiometry, the particle growth processes that occur during ligand removal may differ from one support to another, yielding substantially different catalysts. The dendrimer templating method does not rely on particles growing on the surface, thus reduces the influence of this processing step on the ultimate catalyst, and offering better opportunities for more directly studying support effects.

3.6. Comparisons between mono- and bimetallic catalysts

The primary purpose of this study was to evaluate the viability of DENs as precursors for studying support effects in nanoparticle based catalysts. Catalytic data from both the

mono- and bimetallic catalysts show that DENs are indeed suitable precursors as catalysts with similar CO adsorption and oxidation properties were prepared. This is particularly important for the bimetallic catalysts because other routes do not necessarily yield comparable catalysts on different supports [67]. For the Pt and Pt–Au systems, the support effects were found to be small and differences in support played only a minor role in modulating the nanoparticles' activity. It is therefore not appropriate to undertake a detailed discussion of the potential causes of those relatively small changes in activity. General comparisons between the Pt and Pt–Au systems are of value, however.

The observed synergy for the bimetallic catalysts, as well as the lower E_{app} values, indicates that the catalytic activity cannot be solely attributed to either metal. This does not, however, necessarily indicate that the reaction mechanism is fundamentally different over the bimetallic catalysts. E_{app} values are strongly dependant on heats of adsorption [82–85], so a lower E_{app} may simply reflect a change in adsorption energies upon alloying, rather than a substantial shift in mechanism. The lower E_{app} for the bimetallic catalysts does, however, provide further confirmation that bimetallic nanoparticles remain after dendrimer removal, and implicates bimetallic ensembles as important contributors to the catalysis.

There was no correlation between catalytic activity and the stretching frequency for CO adsorbed on the bimetallic catalysts. The infrared data conclusively show that Au provides new adsorption sites that bind CO much more weakly than the Pt-only catalysts. However, this is not sufficient to implicate Au-based CO adsorption sites as necessarily taking part in the catalysis. The study by Amiridis and co-workers, for example, showed that Pt–Au nanoparticles on silica were relatively inactive catalysts even though they showed Au–CO bands in the IR [67]. In their words, the presence of Au small nanoparticles is “necessary but not sufficient” to prepare active catalysts [67]. It is possible that Au primarily serves to activate oxygen (and cannot do so in some cases), or that Pt is the primary active component and Au activates the reaction over smaller Pt or bimetallic Pt–Au ensembles. The coexistence of surface Pt and Au also breaks up Pt islands [79], which has been suggested as a means of activating key intermediates in the reaction mechanism that are not readily observed with infrared spectroscopy [86,87]. Differences in particle morphologies may also play a role in modifying activity from one support to another, as Bus and van Bokhoven have shown for Pt–Au nanoparticles [80]. In an additional example, Neurock and co-worker have used Monte-Carlo simulations of Pt–Au particles to show that the local arrangement of atoms might be critical for defining the most active NO decomposition sites [15].

4. Summary and conclusions

DENs were used to prepare new supported mono- and bimetallic catalysts on several oxide supports (silica, alumina, titania). Deposition pH was adjusted so that the DENs spontaneously adsorbed onto each support. Control experiments with empty dendrimers indicated that the DEN

adsorption is driven primarily by nanoparticle-support interactions. Active catalysts were prepared by removing the dendrimer with calcination and subsequent reduction at 300 °C. Spectra of CO on the bimetallic catalysts showed that both surface Pt and Au atoms were present after dendrimer removal. Changes in band intensity during CO desorption experiments showed substantial interaction between CO molecules adsorbed on Pt and Au sites, confirming the presence of bimetallic nanoparticles.

The CO oxidation catalysis data indicated catalysis occurred on the metal nanoparticles, and that the support played a small role in modulating the catalytic activity. The bimetallic catalysts were all more active than the monometallic catalysts and had lower apparent activation energies. Pt–Au/_{p25}TiO₂ showed resistance to deactivation during an extended high temperature oxidation treatment. Bimetallic catalyst activities were slightly more sensitive to the support identity than the Pt catalysts and showed no correlation between the CO stretching frequency and catalytic activity. Comparisons with the monometallic materials indicated that the catalytically active site likely involves a bimetallic Pt–Au ensemble.

Acknowledgements

We gratefully acknowledge the Robert A. Welch Foundation (Grant number W-1552) and the U.S. National Science Foundation (Grant number CHE-0449549) for financial support of this work. BJA also thanks the Welch Foundation's Departmental Grant program (W-0031) for a summer stipend and the Beckman Foundation for support during the academic year. Acknowledgement is made to the donors of the American Chemical Society's Petroleum Research Fund for supporting the purchase of the CO oxidation reactor system.

Appendix A. Supplementary data

Supplementary data associated with this article can be found, in the online version, at [doi:10.1016/j.apcatb.2007.12.012](https://doi.org/10.1016/j.apcatb.2007.12.012).

References

- [1] G.C. Bond, D.T. Thompson, *Catal. Rev. Sci. Eng.* 41 (1999) 319–388.
- [2] O. Alexeev, B.C. Gates, *Ind. Eng. Chem. Res.* 42 (2003) 1571–1587.
- [3] R.M. Rioux, S. H. J.D. Hoefelmeyer, P. Yang, G.A. Somorjai, *J. Phys. Chem. B* 109 (2005) 2192–2202.
- [4] R. Narayanan, M.A. El-Sayed, *J. Am. Chem. Soc.* 126 (2004) 7194–7195.
- [5] R. Narayanan, M.A. El-Sayed, *J. Phys. Chem. B* 109 (2005) 12663–12676.
- [6] J. Greeley, M. Mavrikakis, *Nat. Mater.* 3 (2004) 810–815.
- [7] M. Neurock, *J. Catal.* 216 (2003) 73–88.
- [8] J.R. Kitchin, J.K. Nørskov, M.A. Barteau, J.G. Chen, *Phys. Rev. Lett.* 93 (2004) 156801.
- [9] F. Besenbacher, I. Chorkendorff, B.S. Clausen, B. Hammer, A.M. Molenbroek, J.K. Nørskov, I. Stensgaard, *Science* 279 (1998) 1913–1915.
- [10] J. Knudsen, A.U. Nilekar, R.T. Vang, J. Schnadt, E.L. Kunkes, J.A. Dumesic, M. Mavrikakis, F. Besenbacher, *J. Am. Chem. Soc.* 129 (2007) 6485–6490.
- [11] A.L. Allred, *J. Inorg. Nucl. Chem.* 17 (1961) 215.
- [12] C. Mihut, C. Descorme, D. Duprez, M.D. Amiridis, *J. Catal.* 212 (2003) 125–135.
- [13] A. Vazquez-Zavala, J. Garcia-Gomez, A. Gomez-Cortes, *Appl. Surf. Sci.* 167 (2000) 177–183.
- [14] J. Shen, J.M. Hill, M.W. Ramachandra, S.G. Podkolzin, J.A. Dumesic, *Catal. Lett.* 60 (1999) 1–9.
- [15] L.D. Kieken, M. Neurock, D. Mei, *J. Phys. Chem. B* 109 (2005) 2234–2244.
- [16] Y. Lou, M.M. Maye, L. Han, J. Luo, C.J. Zhong, *Chem. Commun.* 5 (2001) 473.
- [17] D. Mott, J. Luo, P.N. Njoki, Y. Lin, L. Wang, C.-J. Zhong, *Catal. Today* 122 (2007) 378–385.
- [18] P. Hernandez-Fernandez, S. Rojas, P. Ocon, J.L. Gomez de la Fuente, J. San Fabian, J. Sanza, M.A. Pena, F.J. Garcia-Garcia, P. Terreros, J.L.G. Fierro, *J. Phys. Chem. C* 111 (2007) 2913–2923.
- [19] A. Habrioux, E. Sibert, K. Servat, W. Vogel, K.B. Kokoh, N. Alonso-Vante, *J. Phys. Chem. B* 111 (2007) 10329–10333.
- [20] D.C. Skelton, H. Wang, R.G. Tobin, D.K. Lambert, C.L. Dimaggio, G.B. Fisher, *J. Phys. Chem. B* 105 (2001) 204–209.
- [21] W.Q. Tian, M. Ge, F. Gu, Y. Aoki, *J. Phys. Chem. A* 109 (2005) 9860–9866.
- [22] C. Song, Q. Ge, L. Wang, *J. Phys. Chem. B* 109 (2005) 22341–22350.
- [23] R. Bouwman, W.H.M. Sachtler, *J. Catal.* 19 (1970) 127.
- [24] H. Okamoto, T.B. Massalski, *Bull. Alloy Phase Diagr.* 6 (1985) 46–56.
- [25] J. Schwank, K. Balakrishnan, A. Sachdev, in: L. Gucci, F. Solymosi (Eds.), *New Frontiers in Catalysis: Proceedings of the 10th International Congress on Catalysis*, Elsevier, Amsterdam, 1993, pp. 905–918.
- [26] B.D. Chandler, A.B. Schabel, C.F. Blanford, L.H. Pignolet, *J. Catal.* (1999) 367–383.
- [27] K. Balakrishnan, A. Sachdev, J. Schwank, *J. Catal.* 121 (1990) 441–445.
- [28] A. Sachdev, J. Schwank, *J. Catal.* 120 (1989) 353–369.
- [29] G. Riah, D. Guillemot, M. Polisset-Thfoin, A.A. Khodadadi, J. Fraissard, *Catal. Today* 72 (2002) 115–121.
- [30] B.D. Chandler, L.I. Rubinstein, L.H. Pignolet, *J. Mol. Catal. A Chem.* 133 (1998) 267–282.
- [31] Y.Z. Yuan, K. Asakura, H.L. Wan, K.R. Tsai, Y. Iwasawa, *J. Mol. Catal. A Chem.* 122 (1997) 147–157.
- [32] Y.Z. Yuan, K. Asakura, H.L. Wan, K.R. Tsai, Y. Iwasawa, *Bull. Chem. Soc. Jpn.* 72 (1999) 2643–2653.
- [33] B.D. Chandler, A.B. Schabel, L.H. Pignolet, *J. Phys. Chem. B* 105 (2001) 149–155.
- [34] L.B. Ortiz-Soto, J.R. Monnier, M.D. Amiridis, *Catal. Lett.* 107 (2006) 13–17.
- [35] E. Bus, D.E. Ramaker, J.A. van Bokhoven, *J. Am. Chem. Soc.* 129 (2007) 8094–8102.
- [36] L.H. Pignolet, D.A. Krogstad, in: H. Schmidbaur (Ed.), *Gold: Progress in Chemistry, Biochemistry, and Technology*, Wiley and Sons, Chichester, England, 1999, pp. 429–493.
- [37] M. Brust, M. Walker, D. Bethell, D.J. Schiffrin, R. Whyman, *J. Chem. Soc. Chem. Commun.* (1994) 801–802.
- [38] J. Luo, M.M. Maye, V. Petkov, N.N. Kariuki, L. Wang, P. Njoki, D. Mott, Y. Lin, C.-J. Zhong, *Chem. Mater.* 17 (2005) 3086–3091.
- [39] Y. Luo, M.M. Maye, L. Han, J. Luo, C.J. Zhong, *Chem. Commun.* 5 (2001) 473.
- [40] A. Henglein, *J. Phys. Chem. B* 104 (2000) 2201–2203.
- [41] L. Lu, G. Sun, H. Zhang, H. Wang, S. Xi, J. Hu, Z. Tian, R. Chen, *J. Mater. Chem.* 14 (2004) 1005–1009.
- [42] C.-W. Chen, M. Akashi, *Polym. Adv. Tech.* 10 (1999) 127–133.
- [43] B. Pawelec, A.M. Venezia, V. La Parola, S.V. Thomas, J.L.G. Fierro, *Appl. Catal. A: Gen.* 283 (2005) 165–175.
- [44] R. Esparza, J.A. Ascencio, G. Rosas, J.F. Sanchez Ramirez, U. Pal, R. Perez, *J. Nanosci. Nanotech.* 5 (2005) 641–647.
- [45] N. Toshima, K. Hirakawa, *Polym. J.* 31 (1999) 1127–1132.
- [46] H. Lang, S. Maldonado, K.J. Stevenson, B.D. Chandler, *J. Am. Chem. Soc.* 126 (2004) 12949–12956.
- [47] C.W. Hills, N.H. Mack, R.G. Nuzzo, *J. Phys. Chem. B* 107 (2003) 2626–2636.
- [48] H. Tang, J.H. Chen, M.Y. Wang, L.H. Nie, Y.F. Kuang, S.Z. Yao, *Appl. Catal. A: Gen.* 275 (2004) 43–48.

- [49] M.I. Awad, M.S. El-Deab, T. Ohsaka, *J. Electrochem. Soc.* 154 (2007) B810–B816.
- [50] H. Lang, R.A. May, B.L. Iversen, B.D. Chandler, *J. Am. Chem. Soc.* 125 (2003) 14832–14836.
- [51] H. Lang, R.A. May, B.L. Iversen, B.D. Chandler, in: J. Sowa (Ed.), *Catalysis of Organic Reactions*, Taylor & Francis Group/CRC Press, Boca Raton, FL, 2005, pp. 243–250.
- [52] A. Singh, B.D. Chandler, *Langmuir* 21 (2005) 10776–10782.
- [53] L. Beakley, S. Yost, R. Cheng, B.D. Chandler, *Appl. Catal. A: Gen.* 292 (2005) 124–129.
- [54] J.G. Gilbertson, G. Vijayaraghavan, K.J. Stevenson, B.D. Chandler, *Langmuir* 23 (2007) 11239–11245.
- [55] R.J. Korkosz, J.D. Gilbertson, K.S. Prasifka, B.D. Chandler, *Catal. Today* 122 (2007) 370–377.
- [56] B. Auten, C.J. Crump, A.R. Singh, B.D. Chandler, in: S.R. Schmidt (Ed.), *Catalysis of Organic Reactions*, CRC Press, Boca Raton, FL, 2006, pp. 315–323.
- [57] D.S. Deutsch, G. Lafaye, D. Liu, B. Chandler, C.T. Williams, M.D. Amiridis, *Catal. Lett.* 97 (2004) 139–143.
- [58] N.N. Hoover, B.J. Auten, B.D. Chandler, *J. Phys. Chem. B* 110 (2006) 8606–8612.
- [59] G. Lafaye, A. Siani, P. Marecot, M.D. Amiridis, C.T. Williams, *J. Phys. Chem. B* 110 (2006) 7725–7731.
- [60] R.M. Crooks, M. Zhao, L. Sun, V. Chechik, L.K. Yeung, *Acc. Chem. Res.* 34 (2001) 181–190.
- [61] J.T. Miller, B.L. Mojet, D.E. Ramaker, D.C. Koningsberger, *Catal. Today* 62 (2000) 101–114.
- [62] D.E. Ramaker, J. de Graaf, J.A.R. van Veen, D.C. Koningsberger, *J. Catal.* 203 (2001) 7–17.
- [63] O.M. Wilson, R.W.J. Scott, J.C. Garcia-Martinez, R.M. Crooks, *Chem. Mater.* 16 (2004) 4202–4204.
- [64] J.C. Garcia-Martinez, R.M. Crooks, *J. Am. Chem. Soc.* 126 (2004) 16170–16178.
- [65] D.S. Deutsch, A. Siani, P.T. Fanson, H. Hirata, S. Matsumoto, C.T. Williams, M.D. Amiridis, *J. Phys. Chem. C* 111 (2007) 4246–4255.
- [66] C.J. Crump, J.D. Gilbertson, B.D. Chandler, *Top. Catal.*, in press.
- [67] L.B. Ortiz-Soto, O.S. Alexeev, M.D. Amiridis, *Langmuir* 22 (2006) 3112–3117.
- [68] B.D. Chandler, L.H. Pignolet, *Catal. Today* 65 (2001) 39–50.
- [69] S.D. Deutsch, G. Lafaye, D. Liu, B.D. Chandler, C.T. Williams, M.D. Amiridis, *Catal. Lett.* 97 (2004) 139–143.
- [70] P. Hollins, *Surf. Sci. Rep.* 16 (1992) 51.
- [71] R.W.J. Scott, O.M. Wilson, R.M. Crooks, *J. Phys. Chem. B* 109 (2005) 692–704.
- [72] B.D. Chandler, J.D. Gilbertson, in: L. Gade (Ed.), *Topics in Organometallic Chemistry: Dendrimer Catalysis*, vol. 21, Springer, 2006, pp. 97–120.
- [73] N. Zheng, G.D. Stucky, *J. Am. Chem. Soc.* 128 (2006) 14278–14280.
- [74] E.S. Shpiro, O.P. Tkachenko, N.I. Jaeger, G. Schulz-Ekloff, W. Grünert, *J. Phys. Chem. B* 102 (1998) 3798–3805.
- [75] V.Y. Borovkov, D.R. Luebke, V. Kovalchuk, J.L. d'Itri, *J. Phys. Chem. B* 107 (2003) 5568–5574.
- [76] B.N.J. Persson, F.M. Hoffmann, *J. Electr. Spectr. Relat. Phenom.* 45 (1987) 215.
- [77] G.A. Somorjai, K.S. Hwang, J.S. Parker, *Top. Catal.* 26 (2003) 87–99.
- [78] E.C. Akubuiro, X.E. Verykios, L. Lesnick, *Appl. Catal.* 14 (1985) 215–227.
- [79] C. Mihut, C. Descorme, D. Duprez, M.D. Amiridis, *J. Catal.* 212 (2002) 125–135.
- [80] E. Bus, J.A. van Bokhoven, *J. Phys. Chem. C* 111 (2007) 9761–9768.
- [81] E. Bus, J.A. van Bokhoven, *Phys. Chem. Chem. Phys.* 9 (2007) 2894–2902.
- [82] D.C. Koningsberger, M.K. Oudenhuijzen, J. De Graaf, J.A. Van Bokhoven, D.E. Ramaker, *J. Catal.* 216 (2003) 178–191.
- [83] A. Bourane, D. Bianchi, *J. Catal.* 202 (2001) 34–44.
- [84] J. Szanyi, D.W. Goodman, *J. Phys. Chem.* 98 (1994) 2972–2977.
- [85] J. Szanyi, W.K. Kuhn, D.W. Goodman, *J. Phys. Chem.* 98 (1994) 2978–2981.
- [86] A. Bourane, D. Bianchi, *J. Catal.* 222 (2004) 499–510.
- [87] P.T. Fanson, W.N. Delgass, J. Lauterbach, *J. Catal.* 204 (2001) 35–52.